An Information-Theoretic One-Erasure Coefficient for Gravity:

Finite Counting, Empirical Comparison, and Limits

David Elliman
dave@neusym.ai

Neuro-symbolic Ltd, Gloucestershire, UK

19 August 2026

Abstract

Why is gravity so weak compared with the other interactions? This paper tests whether the dimensionless coefficient in a horizon-fed gravity relation can arise from a finite record structure rather than being fitted as a free parameter. Direct enumeration shows that the leading virtual-gravity process contains exactly one non-unitary service-event slot. Under the paper's named monitoring-and-erasure identification, that slot is billed as one erasure. Together with the independently derived walk support, this gives a leading coefficient $K_{\mathrm{LO}} = 205.554$: no continuous parameter was adjusted to obtain it, and the principal alternative readings of the same ledger are recorded explicitly. A second-order calculation, with its candidate map and decision bar frozen before the comparison, adds one counted term to give $K_{\mathrm{NLO}} = 206.554$.

Both values are compared against $K_{\mathrm{data}} = 206.49$, which is not a measurement of K but a quantity assembled from the QCD anchor, the Hubble rate and the dark-energy fraction. Each of those inputs is soft enough to move K_{data} by more than the 0.031% residual — the anchor by 8.5%, the Hubble tension by 7.8% — and the inherited fine-structure convention leaves a further band of 0.054 in K, comparable to the residual itself. The leading and second-order coefficients therefore cannot be separated by this comparison, and the residual changes sign if the framework's own horizon and dark-energy values replace the observational ones. What the paper claims is a zero-parameter coefficient counted from a finite census, agreeing with the assembled value to better than half a percent against inputs soft at the several-percent level; it does not claim to fix K to three significant figures.

The agreement is conditional on premises as well as on inputs. It depends on the stated identification between the finite record process and far-field gravity, as well as the symmetry and monitoring premises. Later exact channel analysis proves the associated $\mathcal{P}/\mathcal{Q}$-dephasing and binary information ledger, but it does not derive physical invocation, durable export, reset, heat, Landauer equality, or cadence: the event count is not calorimetry. Within the same conditional service model the horizon is computed as $H_0 = 67.2554\,\mathrm{km\,s^{-1}\,Mpc^{-1}}$, rather than inserted observationally, while the proton mass remains the one dimensionful anchor. These results establish consistency, not a premise-free derivation of Newton's constant or an intrinsic Planck scale. The construction also does not yet supply a gravitational action or nonlinear equations of motion. Instead, it reduces that problem to a sequence of concrete matching tasks: a physical field dictionary from the native perturbation space to the metric and matter fields, a native action or equivalent dynamical prescription, and a matter variation supplying the source and identifying the probe metric (Elliman, 2026b). The paper thus presents an auditable conditional coefficient theorem, its empirical comparison, and a precise account of what would be needed to extend it to gravitational dynamics.

Contents

1 Introduction: two debts any account of gravity must pay

Any microscopic account of gravity owes two answers. First, why is gravity weak compared with the other interactions? Second, what microscopic dynamics make geometry respond to stress-energy? These questions are related, but they are not interchangeable. A formula for Newton's constant does not by itself identify the microscopic degrees of freedom, and a proposed microscopic dynamics does not by itself explain the observed normalization.

Misner, Thorne and Wheeler condensed the reciprocity of general relativity into two lines: "Space tells matter how to move. Matter tells space how to curve" (Misner et al., 1973, p. 5). The saying is often attributed to Wheeler alone, not to Einstein. Its first line refers to motion in a given geometry; its second refers to the way stress-energy enters the field equation. A microscopic theory has to account for both directions, as well as for the observed strength of the coupling.

The finite quantum-error-correcting (finite-QEC) substrate addresses these tasks unevenly. It has a concrete proposal for part of the normalization problem: G is read as the inverse density of horizon information, the short-distance end of an induced-gravity bridge is calculated, and the power of the per-tick irreversibility α_0 is counted in a leading graviton loop. For spacetime response it supplies a metric-as-strain map, a full-energy redshift calculation, a conditional Einstein-form argument, and a finite horizon ledger. It does not yet supply a microscopic history measure or a gravitational action. Section 7 makes that limitation mathematical by exhibiting a family of admissible dynamics that the present data do not distinguish.

The direction of explanation is central to this paper. The coefficient calculation does not begin with a gravitational action, a horizon entropy, or the measured value of Newton's constant and work backwards. It begins with the microscopic record grammar, enumerates the permitted transitions, identifies one non-unitary service-event slot, and—under the named monitoring-and-erasure identification—bills that slot as one erasure before the far-field comparison is made:

$$\begin{gathered}\text{record grammar} \longrightarrow \text{allowed transitions} \longrightarrow \text{one-erasure bill},\\ \text{one-erasure bill} \longrightarrow C_{\text{loop}} = \frac{3}{2} \longrightarrow K_{\text{LO}} = 205.554 \longrightarrow K_{\text{NLO}} = 206.554.\end{gathered} \tag{1}$$

It is in this qualified sense that the calculation is bottom-up. This is not a claim that every other quantum-gravity programme is top-down: string theory, loop quantum gravity, and causal-set theory all contain microscopic structures. The narrower distinction concerns normalization. In many programmes the low-energy Newton coupling remains an empirical input, or its observed value is not derived from a finite microscopic census. Here no continuous coefficient is fitted, although the discrete physical identifications, monitoring premises, and far-field bridge remain genuine assumptions, and the proton still supplies the one measured dimensionful anchor. The residual is therefore the empirical landing of a microscopic explanatory chain, not a statistical uncertainty or a premise-free measurement of G. Its size should not be over-read: as Section 5 sets out, the comparison value is assembled from inputs soft at the several-percent level, so the landing establishes that the counted coefficient is not excluded, not that it is measured.

The substrate itself is a finite record architecture rather than a continuum field theory posited at the outset. A local eight-bit register is restricted by a validity predicate; reversible propagation is a coined walk; and non-unitary service events maintain the record code. The construction, notation, audit methodology, and earlier gravity survey are developed elsewhere (Elliman, 2026c,f,e). We use only the pieces needed for the gravity question and define each at first use. The relativity programme is likewise cited rather than rebuilt (Elliman, 2026h).

Every claim below carries one of three grades. **[verified]** marks a finite calculation, source identity, or published result checked by the accompanying verifier. **[proposition]** marks an implication that also needs a named physical identification. **[speculation]** is reserved for an interpretation or target not licensed by the present calculation, and empirical or conventional inputs are marked **[input]**. These labels allow the reader to separate the finite theorem from the physical premises on which its interpretation depends.

Sections 2–4 introduce the substrate and the thermodynamic bridge. Section 5 presents the one-erasure calculation. Sections 6–9 examine alternative readings, limits, falsifiers, and earlier failed claims. Section 10 places the narrower result alongside several quantum-gravity programmes, using their standard reviews. The appendices specify the event convention and the exact reproduction procedure.

2 The substrate in five paragraphs

The record register. A local matter record is an eight-bit word

$$x = (G_0, G_1, LQ, C_0, C_1, I_3, \chi, W) \in \mathbb{F}_2^8. \tag{2}$$

The labels encode generation, lepton/quark type, colour, isospin, chirality, and weak-service bookkeeping. Three Boolean constraints define the valid record space $\mathcal{P}$; all other words form the syndrome complement $\mathcal{Q}$. **[verified]** Direct enumeration gives $|\mathcal{P}| = 48$ and $|\mathcal{Q}| = 208$ out of $2^8 = 256$ words. These are not fitted state counts: they are the complete truth table of the stated predicate.

The terms “valid” and “syndrome” refer to this code predicate, not to an additional catalogue of observed particles. A word in $\mathcal{Q}$ is a record that violates at least one of the three constraints. It becomes physically relevant here only when the walk and the monitoring assumptions identify a transition into $\mathcal{Q}$ as a service event. This separation is useful: the 48/208 arithmetic can be checked without accepting the later interpretation of a monitored return as a gravitational erasure.

The channel census. A primitive single-bit flip X_k either remains in $\mathcal{P}$ or exits to $\mathcal{Q}$. The number of valid words that exit is 16 for each generation bit G_0, G_1, 24 for each colour bit C_0, C_1, and 48 for each of LQ, χ, W. It is 0 for I_3. Thus I_3 is a gauge/free bit for this predicate, while seven channels are live. The asymmetry is operational: a red census box in Fig. 1 means that some valid record is sent into the syndrome complement by that bit flip; the dashed I_3 box displays the computed zero separately.

Each number counts source words in $\mathcal{P}$, not distinct destinations in $\mathcal{Q}$. For example, the value 48 for LQ means that flipping LQ ejects every valid source word, whereas the value 16 for G_0 means that only one third of the valid sources leave the code under that flip. The zero for I_3 means that its flip preserves validity for all 48 sources. These distinctions become important when the walk support is compared with the exit-active support in Section 5.

The reversible walk. Between service events the record evolves by a discrete coined walk

$$\mathcal{W} = \mathcal{S}\mathcal{C}, \tag{3}$$

where $\mathcal{C}$ is the local coin and $\mathcal{S}$ is the shift. The walk is the coherent part of the model: it transports amplitudes and returns a syndrome-bearing state towards the valid subspace. The distinction between transport and the non-unitary service slot determines the power of α_0. The billing convention adopted here does not assign a second factor to the reversible $\mathcal{P} \to \mathcal{Q}$ injection. Interpreting the remaining service slot as a physically exported, reset, thermodynamically costly erasure is a separate premise, not a consequence of the event census.

The QEC service ledger. The monitored dynamics can be written with jump operators

$$L_k = \sqrt{\gamma_k}\,\Pi_{\mathcal{Q}} X_k \Pi_{\mathcal{P}}, \qquad \mathcal{D}[\rho] = \sum_k \left(L_k \rho L_k^\dagger - \frac{1}{2}\{L_k^\dagger L_k, \rho\} \right). \tag{4}$$

The equation is a compact way of saying that a record can leave the valid code through a specified bit channel and that monitoring makes the record basis operational. The continuous Lindblad form is an envelope of a discrete stroboscopic map, not a claim that the substrate is fundamentally continuous.

The per-tick irreversibility. The normalization

$$\sum_k \gamma_k = \alpha_0 \Lambda_{\mathrm{QCD}} \tag{5}$$

is **[verified]** closed under five adopted identifications: identical register defects; a two-dimensional coin; a coin-singlet/S-wave emission channel; a monitored bridge; and walk-active dissipator support. Equipartition is the unique monitored fixed point, replacing an earlier spectral-gap rationale that has been superseded. The normalization is therefore conditional on those five identifications. The far-field summation leg is still inherited, and the Shell-1 convention $\binom{8}{2} = 28$ remains an explicit audit premise. The same service ledger supplies the matter-sector bit weight and the gravity-sector power of α_0 used below.

Event count, record information, and thermodynamic cost. **[verified]** A later exact instrument calculation sharpens the meaning of this premise. Separating the return into $\mathcal{P}$ and $\mathcal{Q}$ outcomes replaces the coherent channel by its $\mathcal{P}/\mathcal{Q}$-dephasing — composition with $\Delta_{\mathcal{P}/\mathcal{Q}}(\rho) = \Pi_{\mathcal{P}}\rho\,\Pi_{\mathcal{P}} + \Pi_{\mathcal{Q}}\rho\,\Pi_{\mathcal{Q}}$, which preserves trace and sector populations while removing cross-sector coherence, and carries no thermodynamic implication by itself — even when the outcome labels are subsequently forgotten. The two channels differ on exactly 4,352 cross-sector matrix-unit contributions. A minimal two-dimensional Stinespring record then carries the exact binary marginal $\mathrm{diag}(p_{\mathcal{P}}, p_{\mathcal{Q}})$. Thus record formation is dynamically consequential and has an exact information ledger.

That theorem has zero thermodynamic authority by itself. The banked audit derives neither physical invocation nor durable record export, a cyclic reset, a carrier Hamiltonian or bath temperature, heat or work, a substrate Landauer bound or equality, an α_0-to-cost map, or the cadence of record production. It also proves that a fixed uniform 1,096-label source with an input-independent record-only kernel cannot reproduce the input-dependent binary target. The two natural eight-address event families likewise fail for every fixed input-independent schedule: the truthful C_p family would require total schedule weight at least 16/15, while the J_p exit family is affine-incompatible. The lawful remaining possibilities are a separately derived input-dependent schedule $w_{x,p}$ on the same carrier, or an enlarged carrier with its entropy recomputed. In this paper, therefore, "one erasure" means one service-event factor under the disclosed erasure premise; it is not a derived calorimetric statement.

Billing-dependency rider. The coefficient algebra in this paper remains a valid conditional calculation, but its physical erasure invocation is *law-dependent*. In the notation of the closed billing audit it assumes the admissible convention B_E; that convention is neither selected nor adopted. The exact record-fate classification is finer than the older headline: a fine-recorded return carries one jump and zero erasures at system-closed/record-open grade, while the twelve-state erased-record subclass carries one jump, one projection, one erasure and one §5.9 bill but does not close the full carrier. Thus jump nilpotence is not a return theorem, and "one erasure equals one jump" survives only as a numerical coincidence. Explicitly stopping the billing branch would leave the conditional equations intact while withholding their unconditional physical invocation. No thermodynamic cost, cadence, reset law, source-bound unit link or physical scale is derived by this rider.

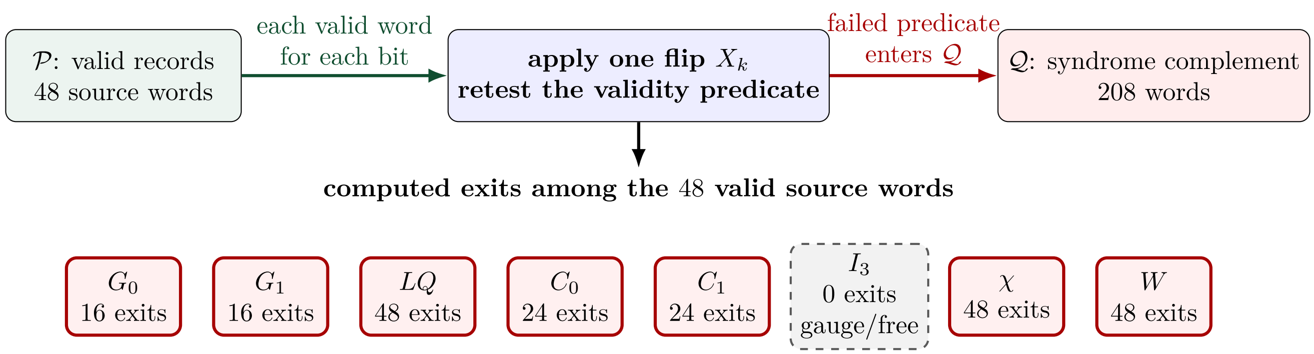

Figure 1: **The eight-bit register and its single-flip exit census.** Derived: the 48/208 split and all eight exit counts. Input: the physical reading assigned to the bit labels and the identification of a $\mathcal{P} \to \mathcal{Q}$ exit as a monitored syndrome event. The dashed I_3 box is a computed zero, not an omitted channel.

3 Gravity as thermodynamics of information

3.1 Jacobson's four ingredients

Jacobson's local thermodynamic argument provides a direct bridge from horizon information to the Einstein equation (Jacobson, 1995). Four ingredients enter.

First, through any spacetime point one considers a small patch of a local Rindler horizon: the causal boundary seen by an accelerated observer. Second, that observer assigns the Unruh temperature T to the horizon. Third, the horizon is assigned an entropy proportional to its area,

$$\mathrm{d}S = \eta\, \mathrm{d}A. \tag{6}$$

Fourth, the Clausius relation

$$\delta Q = T\, \mathrm{d}S \tag{7}$$

is required for every such local horizon, where δQ is the boost-energy flux through it. With local stress-energy conservation, the focusing of the null generators then yields the Einstein equation with a cosmological term.

Newton's constant enters the argument through the entropy density. In conventional units,

$$S_{\mathrm{BH}} = \frac{k_B c^3}{4\hbar G} A, \qquad \eta = \frac{k_B c^3}{4\hbar G}. \tag{8}$$

Thus G is inversely related to the entropy stored per unit area: a larger horizon entropy density corresponds to a smaller gravitational coupling. Put less formally, the more information a square metre of horizon can hold, the weaker gravity is. The entropy–area law gives this relation, but it does not explain why nature chose that storage density (Bekenstein, 1973; Hawking, 1975; Padmanabhan, 2010).

3.2 Equation of state is not microdynamics

Jacobson described the Einstein equation as an equation of state. Boyle's law before the kinetic theory of gases is a useful analogy. A relation such as $PV = Nk_BT$ can be exact and predictive while leaving the underlying constituents, collisions, and nonequilibrium kinetics unknown. In the same way, an Einstein equation obtained from horizon thermodynamics constrains the macroscopic response without identifying the microscopic histories that realize it.

An equation-of-state derivation should therefore neither be dismissed for being macroscopic nor presented as a microscopic quantization of the metric. Thermodynamic laws may be robust emergent results, but their constitutive coefficients and nonequilibrium dynamics are additional questions. The present framework proposes an event ledger and several response maps; the action and the history dynamics remain open.

3.3 The two-scale bridge

The induced-gravity calculation computes the short-distance end of the bridge. A pinned heat-kernel evaluation of the substrate's shear stiffness gives a bare scale of approximately $0.78\,\mathrm{GeV}$, an order-Λ_{QCD} result. The large Planck scale appears only after multiplying by a cosmological horizon-to-lattice factor of order 10^{20} in length. The horizon is now computed inside the conditional service ledger rather than inserted from observation, but the relation remains horizon-mediated. Figure 2 marks that separation visually.

The internalisation is exact within the stated model:

$$r_6 = \frac{(21q_1)^{32}}{21}, \qquad H_0 = \frac{\Lambda_{\rm QCD} r_6}{9\alpha_0}, \qquad M_{\rm P}^2 H_0 = 110\alpha_0^2\Lambda_{\rm QCD}^3. \tag{9}$$

Using the proton mass as the one dimensionful anchor gives $H_0 = 67.2554\,\mathrm{km\,s^{-1}\,Mpc^{-1}}$ and $M_{\rm P} = 1.2208890 \times 10^{19}$ GeV before observational comparison. The result is conditional on the shared $[\mathrm{L3}]/w = 1$ bandwidth premise and on the absence of an additional outside-sector ledger. It removes observed H_0 as an input; it does not generate an absolute scale from nothing.

Three historical formulae in the programme dress this same bridge with different prefactors. They are not independent derivations: all are horizon-mediated and consume $\Lambda_{\rm QCD}$. This consolidation is important because repeated appearances of one large-number relation do not multiply its evidential weight.

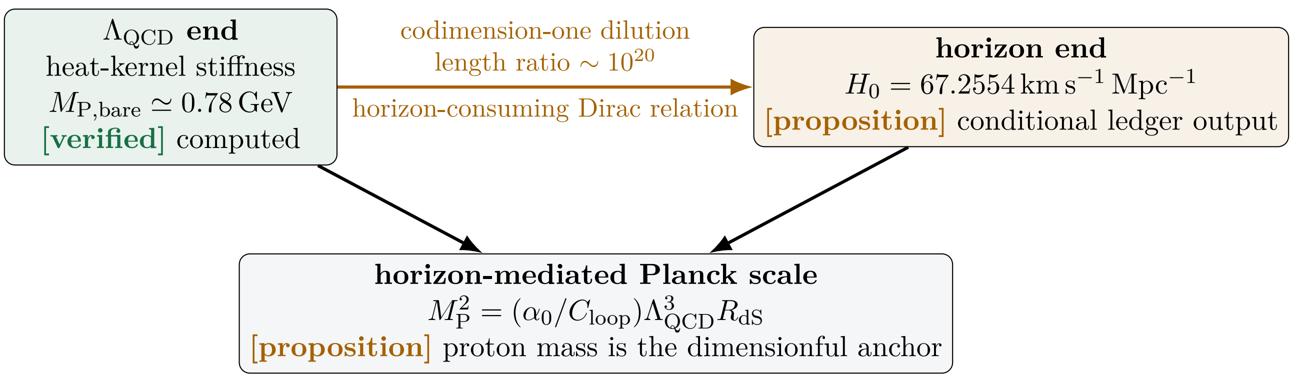

Figure 2: **The two-scale bridge.** Derived: the Λ_{QCD}-end stiffness and the algebraic form of the dilution. Conditional ledger result: the late cosmological horizon, under the shared bandwidth-one premise and outside-sector completeness. The bridge remains a proton-anchored Dirac-class relation among scales, not an intrinsic determination of M_P.

4 What the framework derives about spacetime response

The relativity programme (Elliman, 2026h) separates kinematic response from the absolute gravitational scale. Table 1 gives the current grades. “Computed” means a finite operator or lattice calculation has been executed; “conditional” names the remaining physical identification.

4.1 Metric as strain

For a symmetric strain ϵ, the low-energy momentum transforms as $k \mapsto (I+\epsilon)k$. Therefore

$$E^2 = k^{\mathsf{T}}(I+\epsilon)^2 k = g^{ij}k_i k_j, \qquad g^{ij} = \delta^{ij} + 2\epsilon^{ij} + O(\epsilon^2). \tag{10}$$

The statement is constructive: the same object that deforms the microscopic cone is read macroscopically as the metric perturbation. It does not yet say how ϵ evolves.

4.2 The anti-mass trap and equivalence principle

If strain is coupled only to the bare hopping operator, heavy localized codewords hop less and would gravitate less. That is the anti-mass trap: the putative gravitational charge would measure wavefunction spread rather than total energy. The resolution is to couple the metric to the full energy, including the confinement/Yukawa tension that creates the mass. The resulting redshift is mass-universal in the executed test. The equivalence principle is therefore not assumed by declaring a universal coupling; it is obtained after a wrong, species-dependent coupling is explicitly exposed and rejected.

4.3 The horizon ledger

On the cube graph Q_3, eight vertices are joined by twelve edges and every vertex has degree three. The coboundary of a vertex-label pattern produces a twelve-edge syndrome δ. Its Hamming weight supplies the finite horizon energy ladder. The smallest nonzero cut has weight 3, forced by the degree, while the top cut crosses all 12 edges. Entropy counting, the Hawking ladder, the finite-cell isometry, and the source strain are thus different functionals of one syndrome rather than four unrelated inputs.

4.4 Photon honesty as a worked example

The photon calculation is included as a caution about choosing the object before testing its infrared limit. An early account identified a raw K_6 band with the photon and reported a pass. Power counting in the style of Collins, Perez and Sudarsky first reduced that claim to an unresolved marginal anisotropy. A subsequent object-identity calculation found a more basic problem: the physical photon is the Gauss/Wilson transverse cohomology, whereas the raw K_6 branch fails the Ward/Gauss condition. Once the correct object was used, the apparent cutoff residual disappeared. Propagation above Λ_{QCD} remains a separate framed-null-chain problem with explicit no-go conditions. This history is recorded because a successful test of the wrong object is not evidence for the intended claim.

Target	Claim	Grade	Named conditionality or limit
T-R1	Reversible walk has an isotropic Weyl/Dirac low-energy cone; mass is not a bare hopping term.	**[verified]** computed	Full high-energy continuum completion is not inferred.
T-R2	The physical photon is the Gauss-projected transverse Maxwell cohomology, not the raw K_6 band.	**[verified]** object identity	Trans-Λ_{QCD} quanta require the separately named framed null-chain representation.
T-R3	Strained dispersion gives $g^{ij} = \delta^{ij} + 2\epsilon^{ij} + O(\epsilon^2)$: metric perturbation equals substrate strain.	**[verified]** computed	Leading-order coarse-grained response; not a nonlinear gravitational action.
T-R4	Coupling strain to full energy gives mass-universal redshift and resolves the anti-mass trap.	**[verified]** **[proposition]**	Requires confinement/Yukawa tension in the full stress tensor.
T-R5	Entanglement first law, local KMS service, conserved stress, and linearised Bianchi give the Einstein form.	**[proposition]** conditional theorem	Induced-dominance and leading/local modular-Hamiltonian assumptions; magnitude remains external.
T-R6	Horizon entropy, spectrum, isometry, and source are four readings of one 12-edge strain syndrome δ; $F_{\min} = 3$ follows from 3-regularity.	**[verified]** finite identity	Does not re-derive the area-law coefficient or a fast-scrambling graph.

Table 1: The relativity targets and their current evidential grades.

5 The core result: the coefficient at α_0^1

5.1 The jump channel and finite census

The gravity calculation uses the same valid/syndrome partition as the matter ledger. The primitive algebraic event is a reversible injection from $\mathcal{P}$ to $\mathcal{Q}$, followed by one non-unitary service slot. If N_{event} denotes the number of such slots, the billing factor is

$$\alpha_0^{N_{\text{event}}}, \qquad N_{\text{event}} = 1. \tag{11}$$

Under the named monitoring-and-erasure identification, $N_{\text{erase}} = N_{\text{event}} = 1$. Charging a second factor to the outward Pauli error would count a reversible operation as a second event and would contradict the matter-sector normalization in Eq. (5). This fixes the power of α_0 in the billing model; it does not assign heat to the event.

The census is exhaustive: all 256 words are classified and every bit channel is tested. The I_3 contribution is not merely small; it is exactly absent from the exit census. Consequently, the power of α_0 is fixed by the event convention and the finite calculation rather than inferred from the desired numerical coefficient.

5.2 The one-event theorem and erasure premise

Three statements form the theorem.

T1. [verified] A valid single event carries weight 7/12 on the gate's frozen toy support.

T2. [verified] For every one of the 64 ordered pairs of live channel labels tested in one tick, the double-fire amplitude is exactly zero. Operationally, "exactly zero" means the finite symbolic/rational gate returns the zero element before floating-point comparison; it is not a small numerical residual.

T3. [verified] Across two ticks the two-event contribution is genuinely quadratic: $a_0 = a_1 = 0$ and $a_2 = 45/128$ under the same frozen support. Thus the next event order appears at α_0^2, not as a hidden same-tick correction to the leading coefficient.

Together, T1–T3 give $C_{\text{event}} = 1$ at leading order and an α_0^1 graviton-loop bill. The theorem is conditional on the bandwidth premise, the leading-order effective-field-theory map, the physical monitoring-and-erasure identification, and the empirical far-field comparison. It does not establish a complete quantum-gravity path integral or a thermodynamic cost per event.

The bandwidth premise is shared rather than sector-specific. The gravity coefficient and the separate cosmological-constant ledger both use the same one-active-address-per-tick assumption (the [L3]$/w = 1$ bandwidth lever in the two source ledgers). This is not a second confirmation of the premise: refuting it would strike both sectors at once. It is nevertheless a useful concentration of risk, because one falsification handle replaces two unrelated conditionalities. **[proposition]** Conditional on the monitored-billing axioms and that shared bandwidth-one premise, the stationary dressed cosmological-constant chain is closed at current observational precision (0.10σ); without those premises no cosmological-constant closure is claimed.

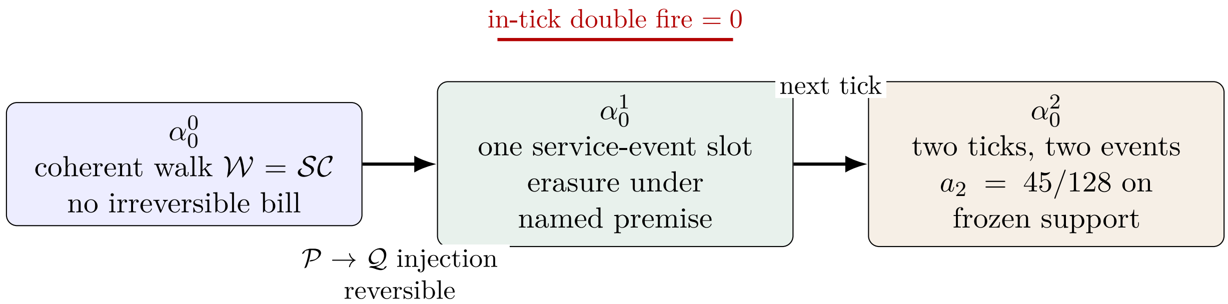

Figure 3: **The billing ladder.** Derived: the coherent/one-event/two-tick order separation, the in-tick zero, and the frozen-support coefficient 45/128. Input: the identification of the non-unitary service slot with a physically invoked, exported and reset graviton-loop erasure. No heat is derived by this ladder.

5.3 $C_{\text{loop}} = 3/2$: support, weights, and competitors

The loop coefficient is fixed before the comparison with K_{data}. Under the shadow premise P-SHADOW, the cited coin, hop, and control-bit definitions give the walk-active support

$$\{C_0, C_1, I_3\}. \tag{12}$$

The I_3 bit is arrowless in the $\mathcal{P} \to \mathcal{Q}$ exit census but remains part of the colourless vacuum-cell walk support. On the nontrivial face-label branch L3-READ, permutation symmetry P-EQUI makes the weights uniform on these three support elements. Two of the three are exit-active, hence

$$\Gamma_{\text{vac}} = \frac{2}{3}\,\alpha_0\Lambda_{\text{QCD}}, \qquad C_{\text{loop}} = \frac{3}{2}, \qquad K_{\text{LO}} = \frac{3}{2\alpha_0} = 205.554. \tag{13}$$

Which constant α_0 is, and which value is used. [input] Equation (13) fits no continuous parameter, but it does inherit one number, and the programme carries two candidates for it. Canon defines α_0 as the *bare* fine-structure constant of the matter–gauge interface, $\alpha_0^{-1} = T(16) + 1 = 137$ exactly. The *dressed* constant from the monitored-endpoint response layer is $\alpha^{-1} = 137.0359991069051$, whose separately pre-registered boundary is $\alpha^{-1}(0) = 137.035999106904$ (Elliman, 2026g). The figure printed above is $\frac{3}{2} \times 137.036$: it uses the dressed constant. The bare reading of the same formula gives $K_{\text{LO}} = 205.500$.

The distinction is not decorative. The two readings differ by 0.0263%, which is 0.054 in K — about 84% of the 0.066 residual reported in Eq. (15) below. Nothing in the present census fixes the choice: the normalization $\sum_k \gamma_k = \alpha_0\Lambda_{\text{QCD}}$ is written with the bare symbol, while the numerical chain evaluates it with the dressed constant. The leading coefficient should therefore be read as carrying a convention band of ± 0.054 in K, and the comparison below is reported with that band in view. Which constant a service normalization inherits is a substrate question this paper does not settle.

Table 2 lists the competing readings considered before the final comparison. They arose from alternative interpretations of the same finite ledger; they were not generated by scanning rational numbers near K_{data}. The reported percentages are deviations from the empirical value in the gate's frozen map.

The uniform-eight support used in an earlier exploratory channel gives $\Gamma = 0.625\alpha_0\Lambda_{\text{QCD}}$, $C_{\text{loop}} = 1.6$, and $K = 219.26$. The support lemma excludes it as walk-derived: it includes channels that the coin/hop/control definitions do not activate. The data therefore select per-bit monitoring in the same basis as the monitored fixed point used in the item-79 normalization, but this is a consistency of two ledgers, not an extra independent measurement.

Weighting/read	C_{loop}	K	miss	Disposition
Walk-active uniform three	3/2	205.554	0.45%	Survivor; support-derived and symmetry-unique under P-SHADOW/P-EQUI/L3-READ.
Touch count	2	274.072	32.7%	Killed by K_{data}.
Per-event level	2	274.072	32.7%	Killed independently; same number, different reading.
Walk support plus χ	4/3	182.715	11.5%	Killed; adds a channel not licensed by the walk support.
Composite-event reading	1	137.036	33.6%	Killed; treats a composite as one primitive bill.

Table 2: The five pre-existing coefficient readings. Agreement is always reported with the competitor denominator.

5.4 The pre-registered second-order landing

The second-order gate froze both the candidate map and the decision bar before evaluation. The required correction was summarized by

$$\kappa_{\text{needed}} = 0.6238. \tag{14}$$

The tested candidates were F1, the walk-active reading with counted $\kappa = 2/3$; F2, the uniform-eight reading with $\kappa = 97/136$; F3, a half-weight reading with $\kappa = 1/2$; and a sign control. The frozen classifications were

Candidate	corrected K	distance within the needed correction	gate outcome
F1 walk-active	206.554	6.9%	LANDS
F2 uniform eight	206.624	14.3%	LANDS
F3 half weight	206.304	19.9%	NEAR
sign control	correct sign	—	PASS

Because both F1 and F2 landed inside the pre-registered bar, the gate's outcome was `LANDS-AMBIGUOUS`. The ambiguity was not resolved by narrowing or moving the bar. It was resolved at the support level: the independent walk-support lemma excludes F2 as a derivation from the stated microscopic walk while retaining F1 under P-SHADOW, P-EQUI, and L3-READ. The resulting comparison is

$$205.554 \longrightarrow 206.554, \qquad K_{\text{data}} = 206.49, \qquad \frac{206.554 - 206.49}{206.49} = 0.031\%. \tag{15}$$

The grade remains *consistent with*. A small residual does not convert an inherited physical identification into a theorem.

What K_{data} is, and how soft it is. [input] The comparison value is not a measurement of K. It is assembled from the same Dirac-class relation as Eq. (17), rearranged:

$$K_{\text{data}} = \frac{\Lambda_{\text{QCD}}^3 R_{\text{dS}}}{M_{\text{P}}^2}, \qquad R_{\text{dS}} = \frac{c}{H_0\sqrt{\Omega_\Lambda}}, \tag{16}$$

evaluated with $\Lambda_{\text{QCD}} = 332\,\text{MeV}$, Planck-2018 $H_0 = 67.36\,\text{km}\,\text{s}^{-1}\,\text{Mpc}^{-1}$ and $\Omega_\Lambda = 0.6847$, and $M_{\text{P}} = 1.2208890 \times 10^{19}\,\text{GeV}$. Those inputs give 206.488, the value quoted above as 206.49.

Every one of those inputs is soft, and each moves K_{data} by more than the residual it is being used to report:

Perturbation	shift in K	vs the 0.066 residual
Dressed for bare α_0 (theory side)	0.054	0.8×
Framework $\Omega_\Lambda = 12\pi/55$ for Planck's 0.6847	0.111	1.7×
Framework $H_0 = 67.2554$ for Planck's 67.36	0.321	4.8×
SH0ES $H_0 = 73.04$ for Planck's 67.36	16.06	243×
Λ_{QCD} per-sector spread 327.1–336.5 MeV	17.52	265×

The last two rows are the dominant floors: the Λ_{QCD} anchor is soft at 8.5% in K, and the Hubble tension spans 7.8%. The move from K_{LO} to K_{NLO}, 0.45% to 0.031%, is some 250 times smaller than the softest of these, so the two orders cannot be separated by this comparison. The defensible reading of Eq. (15) is that the counted second-order term does not spoil an agreement already well inside the input noise — not that it improves a measurement. A prefactor derived to close a residual of this size would be unsupported by the data that define the residual.

Rows two and three deserve particular note, because this paper computes both quantities itself. Substituting the framework's own H_0 and Ω_Λ into Eq. (16) gives $K_{\text{data}} = 206.698$ and turns the $+0.031\%$ residual into -0.069%. A residual that changes sign when the theory's own outputs replace the observational ones is not a quantity to be read at three significant figures, and no weight is placed on its magnitude here.

5.5 The full premise ledger

Figure 4 displays the dependencies of the numerical result. Every root assumption also appears in the text.

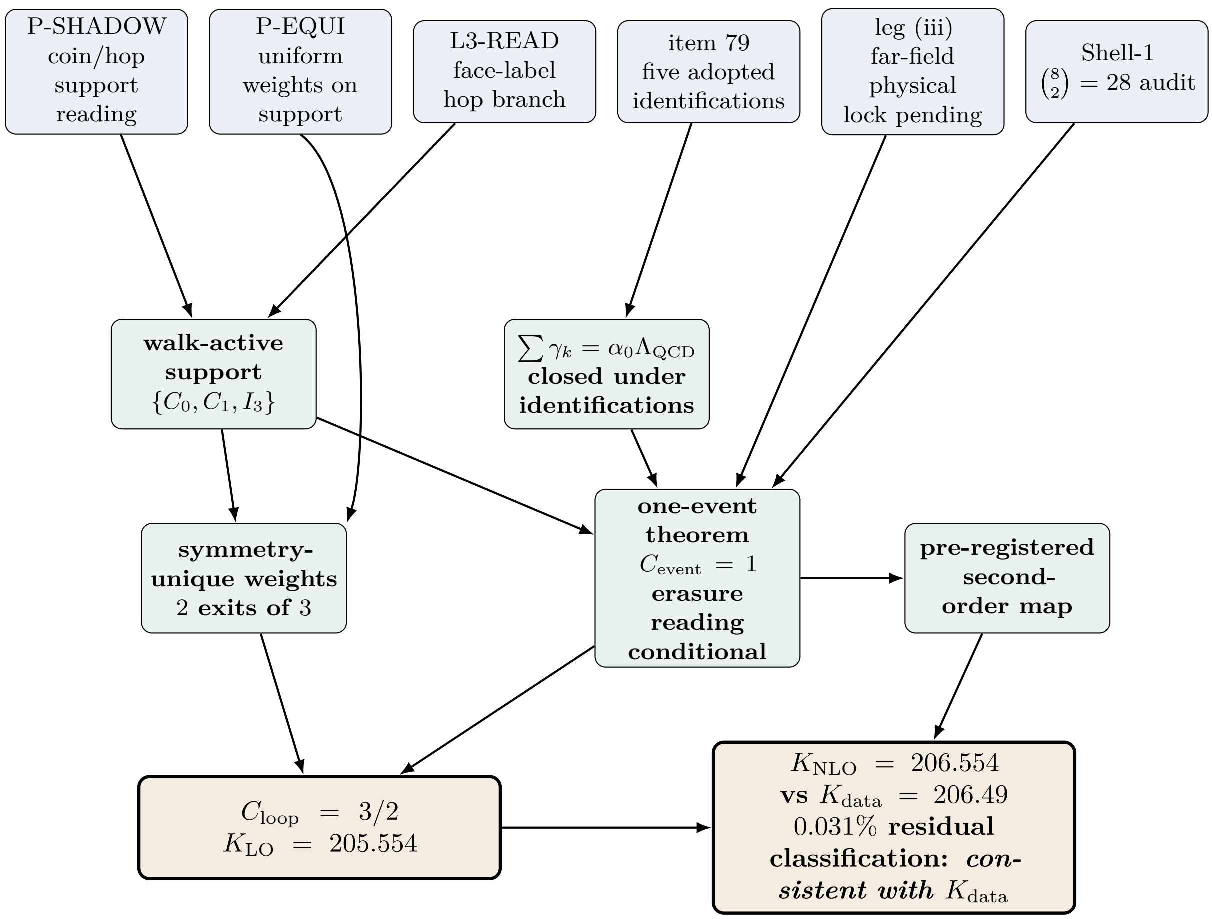

Figure 4: **Premise DAG for the gravity coefficient.** Blue nodes are adopted physical readings or open audits; green nodes are finite theorems conditional on those readings; amber nodes are numerical consequences. The diagram makes the ancestry of the 0.031% landing explicit and prevents that leaf from being quoted as premise-free.

For clarity, item 79's five adopted identifications are: (i) identical register defects; (ii) a two-dimensional coin; (iii) a coin-singlet/S-wave emission channel; (iv) a monitored bridge; and (v) walk-active dissipator support. The other roots are P-SHADOW, P-EQUI, L3-READ, the empirical far-field leg (iii), and the Shell-1 $\binom{8}{2} = 28$ audit. Removing any root weakens a named edge; it does not erase the finite channel census or the in-tick zero.

6 Controls against a numerical coincidence

A close numerical agreement has little evidential value if the formula, support, or comparison rule was chosen after inspecting the target. This section records the controls applied before and after Eq. (15), without assigning the agreement a grade stronger than its inherited premises permit.

6.1 The rationals are counted, not optimized

The small rationals entering the result arise from finite inventories. The two colour channels C_0, C_1 are the two exit-active members of a three-element walk support, producing 2/3 and its reciprocal 3/2. The second-order F1 correction is likewise the counted walk-active value 2/3. The 1/3 complement is visible as the arrowless I_3 share of that support. None of these values was obtained by a continuous fit. In particular, the gate does not search over rational approximants to 206.49.

That fact alone would not suffice. A modeller could invent many finite inventories after seeing the target. The relevant protection is temporal and structural: the candidate map, comparison value, landing bars, and sign control were frozen in the second-order pre-registration; the support lemma was then evaluated independently of the landing. F1 and F2 both landed, so the numerical gate honestly returned `LANDS-AMBIGUOUS`. F2 was removed only because its eight-element support was not produced by the stated walk definitions. The ambiguity was resolved in the model, not by tightening the empirical tolerance.

6.2 Competing readings within the same model

There are five pre-existing coefficient readings in Table 2, plus the exploratory uniform-eight support. The rivals are not generic alternative theories; they are the nearest natural ways to read the same event ledger. Touch counting and per-event counting both give $C_{\text{loop}} = 2$ but remain separate competitors because their semantics differ. Adding χ gives 4/3. Treating the composite as primitive gives 1. Uniform support over eight channels gives 1.6. Their failures range from 11.5% to 33.6%, except for the leading walk-active candidate at 0.45% and the second-order candidates already reported.

Changing the support or the primitive-event convention has a calculable consequence inside this model. The comparison does not range over all possible ultraviolet completions. Under the programme's adversarial protocol, a guard counts as evidence only after a counterexample has been shown to make it fail, and a refusal for an unrelated reason is recorded separately (Elliman, 2026a). The accompanying verifier applies that rule to the four gates used here.

6.3 Two routes that must not be conflated

Two logically distinct computations support the result. The finite register route proves the 48/208 partition, the eight channel exit counts, the in-tick double-fire zero, and the two-tick coefficient. The support route derives $\{C_0, C_1, I_3\}$ and the uniform weighting on its nontrivial branch. Their outputs meet at $C_{\text{event}} = 1$ and $C_{\text{loop}} = 3/2$. They are independent in the limited and auditable sense that neither route reads the other's numerical conclusion as input. They are not two independent theories: both inhabit the same finite-QEC substrate and share the premise ledger in Fig. 4.

The empirical comparison is a third leg, not a derivation. It asks whether the coefficient produced by the two calculations is compatible with the inherited far-field identification. For that reason the numerical grade remains "consistent with." Describing the number as input-free or as measured by the model would overstate the result.

7 The permanent cap and the open dynamics problem

7.1 The T7 bar

The programme's gate T7 records the cap in unusually direct language:

```
HORIZON-CONSUMING -> Dirac-class label MANDATORY and PRESENT
(G7 + rank theorem).  This gate permanently blocks any
'parameter-free M_P prediction' tier.
```

This restriction does not disappear if the numerical agreement improves. Any relation that consumes R_{dS} or H_0^{-1} remains horizon-mediated even when that horizon is computed by the service ledger. The conditional internalisation in Eq. (9) removes observed H_0 as an input, but it does not remove the shared bandwidth-one premise, the outside-sector caveat, or the proton mass as the dimensionful anchor. Better measurements can strengthen the empirical comparison; they cannot turn this relation into an intrinsic or parameter-free Planck scale.

The three historical gravity routes in the programme are consequently consolidated as one Dirac-class family. In schematic form,

$$M_{\text{P}}^2 = \frac{\alpha_0}{C_{\text{loop}}} \Lambda_{\text{QCD}}^3 R_{\text{dS}}. \tag{17}$$

The heat-kernel end supplies a bare scale near $0.78\,\text{GeV}$; the cosmological factor supplies roughly 5×10^{20} in length, or about nineteen to twenty orders of magnitude. Rewriting the hierarchy as information density gives an area count of order

$$\left(\frac{M_{\text{P}}}{\Lambda_{\text{QCD}}}\right)^2 \sim 10^{39} \tag{18}$$

records per strong-scale area, depending on the convention used for Λ_{QCD}. In this form, weak gravity corresponds to a very dense horizon ledger. The service-span construction explains that density only conditionally through the depth-six ledger; it does not derive the proton anchor, prove outside-sector completeness, or evade T7.

7.2 A finite obstruction to selecting dynamics

The missing second debt from the Introduction is not hidden by Eq. (17). A standing-algebra calculation gives

$$\dim \mathcal{F}_3 = \dim \mathcal{I}_3 = 15. \tag{19}$$

The admissible source cone is at least four-dimensional, and after quotienting by overall normalization the projective family is at least three-dimensional. No canonical ray is selected. In representation language, the available graviton-sector orbit contains $6A_{1g}$, whereas ordinary strain decomposes as

$$A_{1g} \oplus E_g \oplus T_{2g}. \tag{20}$$

The existing symmetries therefore do not choose a unique constitutive map from source histories to strain.

The G10 obstruction rules out a unique dynamical conclusion from the present data. No gravitational action, nonlinear field equation, back-reaction law, or microscopic history measure follows from the finite counts alone. A further Hodge or history principle is required. Nine attempted closures are recorded as negative results rather than combined into a preferred answer. The calculation therefore identifies the point at which an additional premise must enter.

7.3 What could close the dynamics gap

The obstruction is useful because it says what another calculation made from the same ingredients cannot accomplish. At the decisive finite witness, the standing-generated algebra already fills the invariant form space: $\dim \mathcal{F}_3 = \dim \mathcal{I}_3 = 15$. Enlarging that algebra with more unrestricted polynomials, or completing the same record/transfer language, cannot reveal a selector that the language does not contain. Indeed, the completed positive source cone has dimension at least four, so even after removing one overall normalization there remain at least three projective directions. The missing information is therefore not another coefficient hidden in the present finite census.

There are three known ways to add the missing information without choosing a preferred answer after inspecting the response. One could derive a microscopic transfer or inertial measure that fixes the relative weights of histories; construct a complete, nonsingular Hodge pairing between the relevant primal and dual record spaces; or supply some other action datum derived independently of the response that it is later asked to explain. The third possibility includes a deliberately disclosed regulator followed by a universality or tuning analysis, but that would define a model rather than derive a unique action from the present substrate alone. Whichever route is taken, the new datum must be frozen before it is compared with the gravitational response.

A separate quantum-measure boundary. The missing gravitational action should not be conflated with the status of the Born measure. A closed-pair ledger explains algebraically why a quadratic valuation arises, but it does not by itself provide the physical probability rule. Within the presently assumed complex-Hilbert/CPTP framework, any preparation map, monitor, and irreversible latch compose to a quantum instrument; calibration forces its outcome effects to be the projectors P_j, returning $p_j = \mathrm{Tr}(P_j\rho)$. Thus no non-circular CPTP construction of literal pair units remains to be found. Gleason remains the physical closure unless the framework introduces an ontic pre-latch net-current register and a local quadratic emission law as genuinely new foundational physics. Neither the doubled closed-time-path notation nor the clonability of orthogonal records after the latch supplies that missing input.

There is a representation-theoretic distinction here, but it separates two different maps. A coefficient attached to each symmetry orbit is fixed by the group and therefore transforms in a copy of the trivial representation. Six orbit coefficients consequently carry $6A_{1g}$, whereas the *linear strain field* carries

$$\mathrm{Sym}^2(V) \cong A_{1g} \oplus E_g \oplus T_{2g}. \tag{21}$$

Schur's lemma therefore gives the true linear statement $\mathrm{Hom}_{O_h}(6A_{1g}, E_g \oplus T_{2g}) = 0$: orbit scalars cannot themselves be a direct linear shear source or order parameter. It does not forbid those scalars from weighting orbit-resolved anisotropic quadratic Hessians. The resulting map is instead from invariant coupling parameters to the three invariant quadratic coefficients (k_A, k_E, k_T). An exact electric-link/magnetic-area calculation, including the cofactor transformation of area pseudovectors, gives such a map with rank three and kernel dimension three. Thus the geometry can span the full cubic stiffness space. This is a conditional bare-affine map; no Hodge or renormalization theorem yet identifies its cone with the induced infrared action. It still selects no action: after normalization its positive image is two-dimensional, and the present inputs choose no point in it. The earlier use of the linear Schur statement to exclude all orbit-indexed quadratic action data was an over-generalized no-go; the remaining obstruction is selection, not representation-theoretic reach.

[verified] A subsequent exact result changes the shape of this limitation without removing it. For a finite-dimensional strict O_h-module V, a positive nonsingular invariant form G, and an equivariant map $J : S \to V$, the pullback on strain is

$$\mathcal{K} = J^*GJ = \sum_{\lambda\in\{A_{1g},E_g,T_{2g}\}} (j_\lambda^* H_\lambda j_\lambda)P_\lambda. \tag{22}$$

The invariant symmetric-form space has dimension exactly three. A positive G cannot create a channel absent from J, and the pullback is covariant under the paired section change $J' = BJ$, $G' = B^{-\mathsf{T}}GB^{-1}$. These are universal representation-theoretic statements, not a physical Hodge datum and not a selector of (k_A, k_E, k_T).

Physical instantiation is now a finite ordered test. C1 must provide the complete correction/coherence and resectioning inventory; C2 must provide the strict active module and exact equivariant retraction; H must provide the positive invariant form and total equivariant J; and the result must then satisfy all 18 identities

$$M_{\lambda o} = j_\lambda^* G_{o,\lambda} j_\lambda \qquad (\lambda \in \{A_{1g}, E_g, T_{2g}\},\ o = 1, \ldots, 6). \tag{23}$$

C1 remains the first unresolved gate. If this chain closes and the induced condition $k_E = k_T$ is thereby licensed on the six-orbit cone, the three quadratic stiffnesses become consequences of the same six couplings used in the gauge action, but their normalized values still fill

$$k_E = k_T, \qquad \frac{5}{2} \le \frac{k_A}{k_E} \le 10. \tag{24}$$

The obstruction has therefore become a gate with a precise pass condition, not a unique action. The segment remains counterfactual and one parameter short of a unique ray. Even a successful pass would establish only a quadratic action up to that remaining ratio; nonlinear equations, matter back-reaction, and the overall magnitude would still require further input, with the latter permanently subject to the T7 horizon-consuming cap. The alternative remains live: the positive cone may be the final statement.

7.4 The strongest licensed statement

The strongest present statement is therefore the conjunction of four clauses:

(i) the Einstein form can be obtained as a conditional equation-of-state theorem;

(ii) the finite substrate supplies a concrete strain variable and a universal full-energy coupling at leading order;

(iii) a leading graviton loop contains one non-unitary service-event factor and, under the named erasure premise, is billed by α_0^1;

(iv) the absolute magnitude is a conditionally internalised, proton-anchored, horizon-fed Dirac relation, while the microscopic dynamics remain open.

Dropping the fourth clause would turn a graded result into an overclaim.

8 Falsification conditions

Table 3 translates the premise diagram into empirical and computational tests. Each criterion states both what would fail and what would remain. In particular, the far-field identification may be rejected without changing the finite event-order theorem.

The locked numerical prediction used by the first row is

$$G_{\text{pred}} = 6.674311 \times 10^{-11}\ \text{m}^3\,\text{kg}^{-1}\,\text{s}^{-2}, \tag{25}$$

reported at $+0.07\sigma$ relative to the comparison available at pre-registration. That current agreement is not banked as timeless: the kill rule activates only when the consensus precision reaches the frozen threshold. CODATA values provide the conventional comparison infrastructure (Tiesinga et al., 2021).

The G-lock and the one-erasure calculation have disjoint premise grammars. The former begins with a proton-mass chain and a frozen ten-candidate junction census; the latter begins with the valid/syndrome register, jump grading, and walk support. They meet only at the empirical gravity comparison. Quoting them as two derivations of one formula would therefore be wrong in both directions: neither supplies a missing premise of the other.

The lunar-ranging line illustrates why scale relations need dynamics. The comparison used here is $H_0 \simeq 6.88 \times 10^{-11}\,\text{yr}^{-1}$ against a bound of $7 \times 10^{-14}\,\text{yr}^{-1}$, a ratio 982.9, rounded to 983. A literal time-varying identification is therefore excluded; a consistent account must explain why the horizon-fed coefficient is adiabatic, screened, or otherwise does not inherit $\dot{R}/R$ directly.

The trans-Λ_{QCD} propagation clause supplies one further dated falsifier. The framed null-chain closure fixes intrinsic vacuum dispersion to exactly zero: invariant counting inside the monitored endpoint action leaves P^2 as the only vacuum quadratic kernel and fixes the endpoint residue to unity, so, writing $\Delta v/c = \zeta_n (E/\Lambda_{\text{QCD}})^n$, every ζ_n vanishes exactly and a nonzero coefficient would be a new endpoint or background operator rather than a correction. The prediction is an exact null, and every published photon-dispersion test is its standing confirmation. Converted to this normalisation, the current strongest 95% confidence nulls are $|\zeta_1| < 3.3 \times 10^{-21}$ (subluminal) from LHAASO's GRB 221009A timing and $|\zeta_1| < 1.5 \times 10^{-23}$ (superluminal) from HAWC, with $|\zeta_2| < 3.5 \times 10^{-25}$ (subluminal, LHAASO) and $|\zeta_2| < 1.2 \times 10^{-31}$ (superluminal, HAWC photon splitting) (Vasileiou et al., 2013; MAGIC Collaboration, 2020; HAWC Collaboration, 2020; LHAASO Collaboration, 2024). Three of the four sign/order quadrants are now bounded more tightly by the published record than by the framework's internal benchmark gates, so the published values are the operative thresholds. The kill is a confirmed, source- and medium-subtracted detection of energy-dependent vacuum photon speed at any order; what dies is the exact-null clause of the endpoint action, while the infrared crystal photon, the in-lattice support wall, and the one-erasure coefficient stand unchanged. Medium-induced or source-intrinsic delays kill nothing: they are ordinary transfer functions.

Clock or instrument	Frozen criterion	What dies	What survives
Newton-G consensus	Once the consensus uncertainty is $\leq$ 15 ppm, a displacement of the locked value by $> 3\sigma$	The G-lock far-field identification and the numerical K_{data} landing	The 48/208 census, event-order theorem, and support counting
FCC-ee electroweak programme	If present central values persist, the C2/N7 alternative row separates from C1 by more than 7σ (forecast is roughly 8–10σ depending on channel)	The losing electroweak normalization branch used elsewhere in the premise network	Gravity's finite channel theorem; the surviving branch must still be propagated explicitly
Lunar laser ranging	Present drift sensitivity bounds a Hubble-scale variation by a factor about 983	Naive $\dot{G}/G \sim H_0$ implementations of the horizon relation	A quasi-static or compensated Dirac relation; the cap remains
Walk-support audit	A source-defined support different from $\{C_0, C_1, I_3\}$, or nonuniform weights without broken symmetry	$C_{\text{loop}} = 3/2$ and the $205.554 \to 206.554$ numerical chain	The one-erasure exponent if the event census remains valid
Register/jump census	Any nonzero in-tick double-fire amplitude, I_3 exit, or more than one non-unitary service slot at leading order	$C_{\text{event}} = 1$ and the α_0^1 event-order theorem	The conditional erasure reading and the thermodynamic interpretation of G as inverse entropy density
History/Hodge construction	A unique, premise-audited source ray and action that contradict the present equation-of-state response	The current response map or its claimed scope	The empirical tests decide which construction survives
GRB photon timing (Fermi-LAT, MAGIC, LHAASO, HAWC)	Any confirmed, source- and medium-subtracted energy-dependent vacuum photon speed, at any order	The exact-null dispersion clause of the framed endpoint action	The IR crystal photon, the in-lattice support wall, and the one-erasure coefficient
Hubble-tension resolution	A confirmed local-distance-ladder H_0 prevailing over the CMB value by more than 3σ against the internalised 67.26	The service-ledger horizon internalisation (conditional Dirac-class)	The one-erasure coefficient, the in-lattice wall, and the vacuum-energy operator map

Table 3: Falsification clocks. The 15-ppm/3σ criterion is frozen in the G-lock pre-registration (Elliman, 2026d); lunar-laser-ranging bounds are compared with the Hubble drift scale using the standard LLR literature (Williams et al., 2004).

9 Failed claims and repairs

Table 4 records claims that were rejected, weakened, or consolidated during the analysis. The register is retained so that the final account does not conceal the alternatives and failed checks that shaped the surviving claim.

Table 4: Failed-claim register.

No.	Earlier claim or shortcut	Counterexample/audit	Present disposition
1	A Brillouin-zone trace fixes $K_{\mathrm{eff}} = 205$.	The trace is not the same object as the monitored event ledger and does not close the physical identifications.	Negative result; not used in the coefficient chain.
2	The raw photon branch passed the infrared test.	The physical state had not been projected into the Gauss/Wilson transverse cohomology.	PASS retracted.
3	Power counting alone established the photon identification.	The Collins–Perez–Sudarsky audit left a marginal anisotropy operator.	Downgraded to an open problem before the object correction.
4	A raw K_6 band is the photon.	It fails the Ward/Gauss condition; the comparison was category-wrong.	Replaced by the transverse cohomology object.
5	An item-131 equation-of-state row inherited a valid L3 reading.	The $w(a)$ claim did not follow from the named branch and survived only through inherited wording.	Killed; no cosmological equation of state is claimed here.
6	Standing algebra selects the gravitational action.	Nine action/Hodge attempts leave a source cone of dimension at least four and no canonical ray.	Registered G10 no-go family; new history input required.
7	D24–D26 were three independent gravity routes.	All three share one emission-order defect and one horizon-consuming large-number bridge (G13).	Consolidated as one Dirac-class family.
8	Item 79's normalization was premise-free.	A 14 August 2026 audit exposed five adopted identifications and stale wording.	Wording corrected; all five premises listed in Sec. 5.
9	A T2 guard demonstrated nontrivial support.	The guard could not be made to fail and was therefore vacuous.	Removed/replaced by a biting support adversary.
10	The pre-registered gate uniquely selected F1.	F2 also landed inside the frozen bar.	Outcome honestly recorded as `LANDS-AMBIGUOUS`; F2 later excluded by support.
11	A leading graviton loop should carry α_0^2 because it has an outward and return leg.	The outward Pauli injection is reversible; all 64 in-tick double-fire amplitudes vanish.	Double-event billing killed; leading order is α_0^1. This event-order result is not calorimetry.

No.	Earlier claim or shortcut	Counterexample/audit	Present disposition
12	A small residual can stand in for a derivation.	Rival supports and premise removal change the result; the far-field leg remains empirical.	Numerical grade fixed at "consistent with."
13	Three similar formulae give threefold evidence for the hierarchy.	Their dependency graphs merge at the same Λ_{QCD}–horizon bridge.	Evidence counted once.
14	A finite source inventory automatically defines back-reaction.	$\dim \mathcal{F}_3 = \dim \mathcal{I}_3 = 15$ but the admissible source family is nonunique.	No action, equation of motion, or back-reaction law inferred.
15	Since $\mathrm{Hom}_{O_h}(6A_{1g}, E_g \oplus T_{2g}) = 0$, orbit-indexed couplings cannot determine any quadratic shear stiffness.	The exact electric-link/magnetic-area cofactor calculation maps the six invariant coefficients to (k_A, k_E, k_T) with rank three.	Over-generalized no-go retracted: the linear-source theorem survives, while the quadratic action problem remains underdetermined because no ray is selected.
16	The undressed handoff chain's tick-13 landing selected a physical dwell or latch for the cosmological-constant branch.	Tick 13 was the undressed trajectory's momentary passage through the true dressed fixed point: $1.0006 \to 1.616$ undressed, whereas the dressed chain gives $0.624 \to 1.0019$.	Coincidence; the demotion is entrenched. The stationary dressed fixed point, not a timing latch, carries the conditional closure.
17	Forming a monitored record automatically establishes a thermodynamic erasure cost.	Exact outcome separation produces $\mathcal{P}/\mathcal{Q}$-dephasing and a binary information ledger, but countermodels and the closed premise audit derive no invocation, durable export, cyclic reset, heat, Landauer equality, α_0 cost map, or cadence.	Record information is derived; physical record cost remains open. "One erasure" is a disclosed billing premise, not a calorimetric theorem.

A recurring problem was that a check could pass for a reason unrelated to the claim it was meant to test. The verification script therefore records the numerical or textual witness expected from each authorized gate, not merely its exit status. An environment error, such as a missing optional numerical package, is reported as such and is not counted as a scientific rejection.

10 Relation to major quantum-gravity programmes

The following comparison uses standard accounts of each programme rather than the terminology of the present repository. The aim is to locate the question addressed here, not to rank otherwise different research programmes. The finite-QEC result concerns one coefficient and its event interpretation; it is not a complete theory of quantum gravity.

10.1 Historical lineage: induced, thermodynamic, and informational gravity

Dirac's large-number observation turned the hierarchy between particle and cosmological scales into a physical question (Dirac, 1937). Equation (17) belongs to that family: it inherits the large-number relation and adds a finite count for one order-one coefficient and one power of α_0. Sakharov treated gravitational stiffness as a response induced by quantum vacuum fluctuations (Sakharov, 1968). Bekenstein and Hawking supplied the entropy–area and temperature relations that quantify horizon information (Bekenstein, 1973; Hawking, 1975). Wheeler's "it from bit" proposal gave this informational direction a broader conceptual form (Wheeler, 1990). Jacobson later derived the Einstein equation as a local thermodynamic equation of state under explicit assumptions (Jacobson, 1995); related thermodynamic and entropic approaches developed the connection further (Verlinde, 2011; Padmanabhan, 2010).

The present work adds a finite channel ledger in which the leading irreversible event can be counted. It does not derive a new Einstein equation or strengthen Jacobson's macroscopic theorem. Its narrower purpose is to calculate one event coefficient and to expose the premises entering the accompanying Dirac-scale relation.

10.2 String theory

String theory replaces point particles by extended quantum objects and incorporates gravitational, gauge, and matter excitations in one framework. Dualities relate descriptions that appear different in perturbation theory (Polchinski, 1994, 1996). Important achievements include improved ultraviolet behaviour and black-hole microstate calculations in controlled settings. The multiplicity of vacua makes unique, model-independent low-energy predictions difficult (Douglas, 2003), although particular string constructions can still have testable consequences (Baumgart et al., 2025).

The finite-QEC construction starts instead from a finite record code and an operational error ledger. Its α_0 coefficient can be checked by an exhaustive finite calculation, but the construction has no complete microscopic quantum dynamics of gravity. An agreement involving one coefficient does not decide between the two frameworks.

10.3 Loop quantum gravity

Loop quantum gravity is a background-independent, nonperturbative quantization of general relativity. Spin networks provide its kinematic states, and geometric operators such as area and volume have discrete spectra (Rovelli, 1998). In the cited black-hole calculation, boundary-state counting gives an entropy proportional to area and the Immirzi parameter is fixed by the Bekenstein–Hawking normalization (Ashtekar et al., 1998). The finite-QEC horizon ledger resembles this picture in two limited respects: geometric information is discrete, and boundary data carry the horizon count. The present paper does not independently derive the factor 1/4; it enters through the item-22 horizon consistency check rather than through an Immirzi parameter.

The differences are more important than the resemblance. Background independence and the quantum constraint algebra are central to loop quantum gravity. The finite-QEC substrate assumes a preferred discrete service structure and obtains a metric-as-strain response only after coarse graining. That choice gives an explicit operational clock and an auditable finite register, but it leaves background-independent dynamics unfinished. Proposed benefits elsewhere in the programme, including a finite cosmological exhaust ledger and a representation for propagation above Λ_{QCD}, are not re-derived in this paper.

10.4 Asymptotic safety

The asymptotic-safety programme asks whether the renormalization-group flow of gravity approaches a non-Gaussian ultraviolet fixed point with finitely many relevant directions, so that a continuum quantum field theory remains predictive (Niedermaier, 2007; Reuter and Saueressig, 2012). Evidence is sought in the stability of the fixed-point structure under changes of truncation and matter content. The 0.78 GeV induced scale used here is not such a fixed point, and this paper makes no ultraviolet-completion claim. Conversely, asymptotic safety does not supply the finite register interpretation of one erasure. Only a future coarse-grained history theory could determine whether the two descriptions are compatible.

10.5 Causal sets and causal dynamical triangulations

Causal-set theory takes causal order and local finiteness as the primitive data from which continuum spacetime should emerge (Bombelli et al., 1987; Sorkin, 2005). Causal dynamical triangulations instead defines a regulated sum over causally restricted triangulated geometries and studies its phases numerically (Ambjørn et al., 2012). Both replace a fundamental continuum by discrete relational data, but causal sets emphasize order and number, whereas CDT emphasizes an ensemble and its continuum limit.

The finite-QEC substrate is also discrete, but its primitive data are error-corrected records and service histories rather than causal order or simplicial geometry. It has a complete census of its local predicate and no corresponding ensemble or history measure. The G10 obstruction identifies the need for such a dynamical principle; it does not provide one.

10.6 Emergent and entropic gravity

Thermodynamic and entropic approaches interpret gravity as the macroscopic response of microscopic degrees of freedom (Jacobson, 1995; Verlinde, 2011; Padmanabhan, 2010). This is the closest comparison. The additional proposal here is that one service-event factor can be counted in both a matter ledger and a leading graviton-loop ledger. The count is conditional on P-SHADOW, P-EQUI, L3-READ, the five item-79 identifications, the far-field comparison, and Shell-1. Its interpretation as thermodynamic erasure carries the additional invocation/export/reset premises stated above. Those assumptions are part of the result and cannot be suppressed under the general label "emergent gravity."

10.7 Open lemmas

Two structural links remain open. First, the Grassmann-trace shadow must turn the finite standing algebra into a justified continuum source functional. Second, the L3-READ face-label hop must follow from the microscopic history rule rather than merely being compatible with the walk. The former far-field counting link has advanced: the service ledger now establishes

$$r_6 N_{\text{lock}} = 9\alpha_0 \tag{26}$$

with its required normalization and without using observed H_0 as an input. Its physical identification with the cosmological horizon remains conditional on the shared bandwidth-one premise and outside-sector completeness. These remaining conditions are coupled to G7's far-field comparison and G10's source-ray obstruction. A successful action/history measure must discharge them together or explain why one is unnecessary.

Programme	Primitive emphasis	Principal gravity achievement	Contrast with this paper
String theory	Extended quantum objects and duality	UV-complete quantum gravity in controlled constructions	Far more complete dynamics; less direct finite coefficient ledger
Loop quantum gravity	Background-independent quantum geometry	Discrete area/volume and horizon state counting	Similar discreteness; different clock, constraints, and background status
Asymptotic safety	Continuum RG fixed point	Candidate predictive UV completion	Fixed-point dynamics versus finite operational erasure count
Causal sets	Causal order and local finiteness	Discrete causal kinematics and covariant growth questions	Order/number versus record validity and service
CDT	Causal triangulation ensemble	Nonperturbative emergent spacetime phases	Has a history ensemble; this substrate presently does not
Emergent/entropic gravity	Horizon thermodynamics/information	Einstein equation as equation of state	Closest lineage; this paper adds a finite one-event bill

Table 5: A question-oriented comparison, based on the cited standard reviews.

11 Conclusion

The paper began by separating the normalization of gravity from the microscopic dynamics of geometry. The finite-QEC substrate gives a graded answer to part of the first question and a finite obstruction to answering the second with the present assumptions.

The exact finite result is simple to state. Of 256 eight-bit words, 48 are valid and 208 are syndrome words. Seven bit channels can leave the valid space; I_3 cannot. A leading virtual graviton-loop event is a reversible injection followed by one non-unitary service slot. All 64 tested in-tick double fires vanish exactly, while the next two-event contribution appears across two ticks with $a_0 = a_1 = 0$ and $a_2 = 45/128$. The leading bill is therefore α_0^1; identifying that slot as a physically exported, reset erasure remains a named premise.

Under the stated walk-support and symmetry premises, two exit-active channels among three support elements give $\Gamma_{\text{vac}} = (2/3)\alpha_0\Lambda_{\text{QCD}}$ and $C_{\text{loop}} = 3/2$. The leading numerical value 205.554 is not alone: among five pre-existing weighting readings, four structural rivals miss the comparison by 11.5%–33.6%, and of two support choices the exploratory eight-support reading is excluded by the walk. A frozen second-order gate moves the surviving result to 206.554 against 206.49. The 0.031% residual is notable, but its grade is and remains "consistent with."

In the information-theoretic reading, Newton's constant is inversely related to the entropy density of local horizons, so weak gravity corresponds to a dense horizon ledger. The same service-event factor weights the matter process and the leading gravity loop. The proposed link is therefore operational: two coefficients count the same event, rather than being equated as unexplained formulae. Exact $\mathcal{P}/\mathcal{Q}$-dephasing proves that forming the corresponding binary record changes the channel, but it does not yet prove the event's thermodynamic cost or cadence.

The limits are part of the conclusion. The service ledger now computes the horizon entering the relation, but only conditionally on the shared bandwidth-one premise and outside-sector completeness; the proton mass remains the one dimensionful anchor. The absolute scale is therefore still a horizon-mediated Dirac-class relation rather than an intrinsic or parameter-free Planck-mass prediction. The standing algebra selects no unique source ray, so no action, nonlinear equation of motion, or back-reaction law has been derived. The universal pullback bridge now turns that obstruction into the ordered $C1 \to C2 \to H$ factorisation gate, but C1 remains unresolved and the possible $5/2 \leq k_A/k_E \leq 10$ segment remains counterfactual. Progress requires that gate to close without importing the desired stiffnesses, while also deriving the face-label reading and far-field lemma and reproducing the finite response ledger without assuming its conclusion.

The methodological contribution is the combination of a finite theorem, a competitor census, a record of failed claims, dated falsifiers, and a permanent limit on the conclusion. If the numerical agreement survives improved measurements and a satisfactory dynamics is found, the one-erasure ledger would provide a microscopic account of part of the gravitational normalization. If not, the finite calculations will still locate the point at which the proposed bridge fails.

A Register predicate and event convention

The local record domain is $\mathbb{F}_2^8$ with coordinate order

$$(G_0, G_1, LQ, C_0, C_1, I_3, \chi, W). \tag{27}$$

The executable validity predicate is the authority for membership in $\mathcal{P}$; this paper intentionally does not replace it with an informal Boolean paraphrase that could drift. Appendix B identifies the exact gate source and commit. The verifier re-enumerates all words through that gate and checks the census $48 + 208 = 256$ and the exit vector

$$(16, 16, 48, 24, 24, 0, 48, 48). \tag{28}$$

A primitive algebraic event is counted only at the non-unitary service slot. Coherent injection $\Pi_{\mathcal{Q}} X_k \Pi_{\mathcal{P}}$ identifies an error channel but does not independently earn a second factor. "One event" therefore means one service slot, not one outward operator plus one return operator. Calling that slot an erasure additionally assumes physical invocation, record export and reset. The exact $\mathcal{P}/\mathcal{Q}$-dephasing establishes information transfer but not heat, a Landauer equality, an α_0 cost map, or cadence. The event convention is shared with the matter normalization; changing it must change both ledgers.

The grades used in the paper are closed:

[verified] exact finite output, source identity, or directly checked bibliographic fact;

[proposition] implication relative to named physical premises;

[input] empirical or conventional quantity consumed by the argument;

[speculation] unlicensed target, interpretation, or future construction.

No unmarked numerical agreement is intended to carry a stronger grade than the sentence surrounding it.

B Authorized gate ledger

Exactly four executable physics gates are authorized for this paper. Table 6 binds the source path, repository commit, source SHA-256, and successful exit. The verifier reruns these four and no other physics gate.

Table 6: Exact gate identities.

Gate	Commit	Source SHA-256	Exit
`fact_c_one_contact_one_tick_gate.py`	`7d331b5cc3c2`	`8109eb529fbb0fcd12d82cbf9dadb5ccdacac4ae012f2ee01273050d51a4f8fe`	0
`gravity_second_order_billing_prereg_gate.py`	`2d7a7418eec0`	`104823bd57192eae23fdbcfaea9bdba35a29497128fde3dc86f6cbde21f458f6`	0
`gamma_from_walk_support_lemma_gate.py`	`9a05fce5af29`	`701ac5031aad814bdd1b151a28b9d4dad5c6a5911524c474dd57dccd41b857ca`	0
`item119_jump_channel.py`	`e34c797b5e8e`	`87d38df066836abc57803f97edac0f31fd83570648ae93c13581d4d393b90a54`	0

The first three gates run with the repository's ordinary Python interpreter. The fourth imports NumPy. On the writing host, the base interpreter lacked NumPy and failed before any scientific assertion; that environment failure is not evidence. The successful ledger entry was produced with the bundled dependency interpreter and NumPy 2.3.5. The verifier locates a NumPy-capable interpreter explicitly and refuses if one is unavailable.

The key expected witnesses are: 48/208 words, exit counts $16, 16, 48, 24, 24, 0, 48, 48$, 64 exact in-tick zeros, event weight 7/12, and $(a_0, a_1, a_2) = (0, 0, 45/128)$ from the first gate; F1/F2/F3 corrected values $206.554, 206.624, 206.304$ with outcome `LANDS-AMBIGUOUS` from the second; support $\{C_0, C_1, I_3\}$ and the competitor table from the third; and the independent dissipative/jump and quadratic-residual checks from the fourth.

Supporting banked records. Eight later records update the limitation and dependency discussion without becoming extra coefficient gates. The universal pullback report was banked at `ed67669`, has report id `39bb77abdc94a094616f5a0d2bdf0e31c67d3bdee3d6077c787a16cc04ccac6f`, and was entered into canon at `12aea7b`. The observational-noise-floor closure is bound to `cc_residual_noise_floor.py` at `3313b5554e2d`; the shared-bandwidth and tick-13 audit is bound to `cc_clause_ii_bandwidth_identity_gate.py` at `da5c772cd6f0`; and the horizon internalisation is bound to `horizon_service_span_internalisation_results.json` at `bc324e8`. The record/instrument boundary is bound successively to the T3C, T3R, T3RB and T3MU reports at `77f7cee`, `4bc0877`, `839d0e9` and `d72e964`. The verifier checks their committed identities and the exact stored claims used here. They are not counted as independent derivations of the one-erasure coefficient.

C Reproduction protocol

From the repository root, the paper can be checked with

```
python3 recent_papers/gravity_one_erasure/verify_gravity_paper.py
make -C recent_papers/gravity_one_erasure pdf
```

The verifier checks source identities, reruns exactly the four gates in Appendix B, pins the eight supporting banked records named above, asserts the numerical witnesses quoted in the text, validates the required bibliography records, and scans the source for the claim grades and permanent cap. A zero exit means those checks passed; it does not certify the physical premises.

The PDF target runs `pdflatex`, `bibtex`, and two further `pdflatex` passes. The source contains no external graphics: all four figures are TikZ and are therefore reproduced from the reviewed text. Reproducers should inspect the log for undefined citations or references after the final pass.

Code availability

The verification program used for this paper is `verify_gravity_paper.py`. It checks the cited source identities, reruns the four authorized physics gates, pins the eight supporting banked records used in the updated limitations, validates the numerical witnesses and premise disclosures, and checks the bibliography against the certified key set. The version submitted with the manuscript will be preserved as a versioned Zenodo software record so that the cited code cannot change in place. **TODO (owner): publish the prepared Zenodo deposit, add its version DOI to `references.bib`, and cite that record here before submission.**

Acknowledgements

TODO (owner): add acknowledgements and disclosure of machine-assisted drafting/review before publication.

References

Jan Ambjørn, Jerzy Jurkiewicz, and Renate Loll. Causal dynamical triangulations and the quest for quantum gravity. In Jeff Murugan, Amanda Weltman, and George F. R. Ellis, editors, *Foundations of Space and Time*, pages 321–337. Cambridge University Press, 2012.

A. Ashtekar, J. C. Baez, A. Corichi, and K. Krasnov. Quantum geometry and black hole entropy. *Phys. Rev. Lett.*, 80:904–907, 1998. doi: 10.1103/PhysRevLett.80.904.

Matthew Baumgart, Panagiotis Christeas, Jonathan J. Heckman, and Rebecca J. Hicks. How to falsify string theory at a collider. *Phys. Rev. Research*, 7:023184, 2025. doi: 10.1103/PhysRevResearch.7.023184.

Jacob D. Bekenstein. Black holes and entropy. *Phys. Rev. D*, 7:2333–2346, 1973.

Luca Bombelli, Joohan Lee, David Meyer, and Rafael D. Sorkin. Space-time as a causal set. *Physical Review Letters*, 59(5):521–524, 1987. doi: 10.1103/PhysRevLett.59.521.

Paul A. M. Dirac. The cosmological constants. *Nature*, 139:323, 1937.

Michael R. Douglas. The statistics of string/m theory vacua. *JHEP*, 05:046, 2003. doi: 10.1088/1126-6708/2003/05/046.

David Elliman. Adversarial self-registration: A working protocol for keeping a machine-assisted theory programme honest, 2026a. Record DOI: https://doi.org/10.5281/zenodo.21219212.

David Elliman. C2 algebra and gravitational response: Algebraic structure, continuum obstructions, and observable tests, 2026b. Concept DOI: https://doi.org/10.5281/zenodo.22699107.

David Elliman. Foundations and methodology for a finite-qec substrate: Code, crystallisation, ledgers, and audit protocol, 2026c. Concept DOI: https://doi.org/10.5281/zenodo.20671855.

David Elliman. Newton's constant from the proton mass: A locked zero-parameter prediction, 2026d. Concept DOI: https://doi.org/10.5281/zenodo.21140769.

David Elliman. Gravity, horizons, and black holes in the finite-qec substrate, 2026e. Concept DOI: https://doi.org/10.5281/zenodo.20671863.

David Elliman. A finite-qec substrate program for particle physics and cosmology: Current canon and audit methodology, 2026f. Concept DOI: https://doi.org/10.5281/zenodo.20671921.

David Elliman. A pre-registered fine-structure boundary from a monitored wilson-endpoint response: $\alpha^{-1}(0) = 137.035999106904$, registered mid-fork, 2026g. Concept DOI: https://doi.org/10.5281/zenodo.21221269.

David Elliman. Special and general relativity from the finite-qec substrate: The propagation clock, the equivalence principle, and the horizon ledger, 2026h. Concept DOI: https://doi.org/10.5281/zenodo.20677638.

HAWC Collaboration. Constraints on Lorentz invariance violation from HAWC observations of gamma rays above 100 TeV. *Phys. Rev. Lett.*, 124:131101, 2020. doi: 10.1103/PhysRevLett.124.131101. A. Albert et al.

Stephen W. Hawking. Particle creation by black holes. *Commun. Math. Phys.*, 43:199–220, 1975.

Ted Jacobson. Thermodynamics of spacetime: the Einstein equation of state. *Phys. Rev. Lett.*, 75: 1260–1263, 1995. doi: 10.1103/PhysRevLett.75.1260.

LHAASO Collaboration. Stringent tests of Lorentz invariance violation from LHAASO observations of GRB 221009a. *Phys. Rev. Lett.*, 133:071501, 2024. doi: 10.1103/PhysRevLett.133.071501. Z. Cao et al.

MAGIC Collaboration. Bounds on Lorentz invariance violation from MAGIC observation of GRB 190114c. *Phys. Rev. Lett.*, 125:021301, 2020. doi: 10.1103/PhysRevLett.125.021301. V. A. Acciari et al.

Charles W. Misner, Kip S. Thorne, and John Archibald Wheeler. *Gravitation*. W. H. Freeman, San Francisco, 1973. ISBN 978-0-7167-0344-0.

Max Niedermaier. The asymptotic safety scenario in quantum gravity—an introduction. *Class. Quantum Grav.*, 24:R171–R230, 2007. doi: 10.1088/0264-9381/24/18/R01.

T. Padmanabhan. Thermodynamical aspects of gravity: New insights. *Rep. Prog. Phys.*, 73:046901, 2010. doi: 10.1088/0034-4885/73/4/046901.

Joseph Polchinski. What is string theory?, 1994. Les Houches lectures, report NSF-ITP-94-97.

Joseph Polchinski. String duality. *Rev. Mod. Phys.*, 68:1245–1258, 1996. doi: 10.1103/RevModPhys.68.1245.

Martin Reuter and Frank Saueressig. Quantum einstein gravity. *New J. Phys.*, 14:055022, 2012. doi: 10.1088/1367-2630/14/5/055022.

Carlo Rovelli. Loop quantum gravity. *Living Rev. Relativ.*, 1:1, 1998. doi: 10.12942/lrr-1998-1.

A. D. Sakharov. Vacuum quantum fluctuations in curved space and the theory of gravitation. *Sov. Phys. Dokl.*, 12:1040–1041, 1968. [Dokl. Akad. Nauk SSSR 177, 70 (1967)].

Rafael D. Sorkin. Causal sets: Discrete gravity. In Andrés Gomberoff and Donald Marolf, editors, *Lectures on Quantum Gravity*, pages 305–327. Springer, 2005. doi: 10.1007/0-387-24992-3_7.

Eite Tiesinga, Peter J. Mohr, David B. Newell, and Barry N. Taylor. CODATA recommended values of the fundamental physical constants: 2018. *Rev. Mod. Phys.*, 93:025010, 2021.

V. Vasileiou, A. Jacholkowska, F. Piron, J. Bolmont, C. Couturier, J. Granot, F. W. Stecker, J. Cohen-Tanugi, and F. Longo. Constraints on Lorentz invariance violation from Fermi-Large Area Telescope observations of gamma-ray bursts. *Phys. Rev. D*, 87:122001, 2013. doi: 10.1103/PhysRevD.87.122001.

Erik Verlinde. On the origin of gravity and the laws of Newton. *JHEP*, 04:029, 2011.

John Archibald Wheeler. Information, physics, quantum: the search for links. In Wojciech H. Zurek, editor, *Complexity, Entropy and the Physics of Information*. Addison-Wesley, 1990.

James G. Williams, Slava G. Turyshev, and Dale H. Boggs. Progress in lunar laser ranging tests of relativistic gravity. *Phys. Rev. Lett.*, 93:261101, 2004.